Magnetic properties of the spin S = 1/2 Heisenberg chain with hexamer modulation of exchange

2012 J. Phys.: Condens. Matter 24 116002

(http://iopscience.iop.org/0953-8984/24/11/116002)

IOP PUBLISHING JOURNAL OF PHYSICS: CONDENSED MATTER

J. Phys.: Condens. Matter **24** (2012) 116002 (12pp) doi:10.1088/0953-8984/24/11/116002

Magnetic properties of the spin $S = 1/2$ Heisenberg chain with hexamer modulation of exchange

M Shahri Naseri[1], G I Japaridze[2,3], S Mahdavifar[1] and S Farjami Shayesteh[1]

[1] Department of Physics, University of Guilan, 41335-1914 Rasht, Iran
[2] College of Engineering, Ilia State University, Cholokashvili Avenue 3-5, 0162 Tbilisi, Georgia
[3] Andronikashvili Institute of Physics, Tamarashvili Street 6, 0177 Tbilisi, Georgia

Received 9 October 2011, in final form 12 January 2012
Published 21 February 2012
Online at stacks.iop.org/JPhysCM/24/116002

Abstract
We consider the spin-1/2 Heisenberg chain with alternating spin exchange in the presence of additional modulation of exchange on odd bonds with period 3. We study the ground state magnetic phase diagram of this hexamer spin chain in the limit of very strong antiferromagnetic (AF) exchange on odd bonds using the numerical Lanczos method and bosonization approach. In the limit of strong magnetic field commensurate with the dominating AF exchange, the model is mapped onto an effective XXZ Heisenberg chain in the presence of uniform and spatially modulated fields, which is studied using the standard continuum-limit bosonization approach. In the absence of additional hexamer modulation, the model undergoes a quantum phase transition from a gapped phase into the only one gapless Lüttinger liquid (LL) phase by increasing the magnetic field. In the presence of hexamer modulation, two new gapped phases are identified in the ground state at magnetization equal to $\frac{1}{3}$ and $\frac{2}{3}$ of the saturation value. These phases reveal themselves also in the magnetization curve as plateaus at corresponding values of magnetization. As a result, the magnetic phase diagram of the hexamer chain shows seven different quantum phases, four gapped and three gapless, and the system is characterized by six critical fields which mark quantum phase transitions between the ordered gapped and the LL gapless phases.

(Some figures may appear in colour only in the online journal)

1. Introduction

Plateaus observed in the zero-temperature magnetization curve of spin systems usually display the quantum nature of this phenomenon. Formation of a plateau is connected with the generation of a gap in the excitation spectrum, which can be in some senses regarded as a realization of generation of the Haldane conjecture [1]. The quantum nature of a plateau formation mechanism was clearly shown in the seminal paper by Oshikawa *et al* [2], who proposed the condition for realization of a plateau at magnetization m as $n(S - m) =$ integer, where S is the magnitude of the local spin, n is the number of spins in a translational unit cell of the ground state and m is normalized to 1 at saturation.

A particular realization of such a scenario appears in the one-dimensional (1D) space-modulated (alternating) quantum spin systems. The bond-alternating Heisenberg spin-1/2 chains which are obtained by a space modulation in the exchange couplings represent one particular subclass of low-dimensional quantum magnets which pose interesting theoretical [3–17] and experimental [18–26] problems. The bond alternating spin-1/2 chains have a gap in the spin excitation spectrum and reveal extremely rich quantum behaviors in the presence of an external magnetic field. By turning the magnetic field, the excitation gap reduces and reaches zero at the first critical field. Simultaneously, the magnetization remains zero up to the first critical field. By greater increasing of the magnetic field, the system

remains in the gapless phase and at the second critical field, the gap re-opens and the saturation plateau appears in the magnetization curve. These models have only two plateaus, at zero and saturation values of the magnetization.

The subject of the space-modulated spin chains has grown in recent years and it has been found that a space modulation in the exchange couplings can affect the behaviors of the field-induced magnetization. First, the modulation was suggested as the ferromagnetic–ferromagnetic–antiferromagnetic (F–F–AF) trimerized Heisenberg spin-1/2 chains and found that the magnetization curve has a plateau at 1/3 of the saturation magnetization value [9, 27]. The F–F–AF trimerized chain has been observed experimentally in the compound $3CuCl_2 \cdot 2dx$ [28]. During recent years, the trimerized Heisenberg chains have been studied in detail [29–31]. Using the density matrix renormalization group (DMRG) method, the observation of the plateaus for chains with different spin ($S = 1/2, 1, 3/2, 2$) has been reported [29]. A magnetization plateau at $m = 1/3$ of the saturation value exists at low temperature for both, F–F–AF and AF–AF–F trimerized spin-1/2 chains [30]. The spin structure factors are also calculated for the trimerized cases and found that the static structure factor does not vary with the external magnetic field at the plateau state [31].

The other example of the spin chain with mixed (F–AF) and spatially modulated exchange is the compound $Cu(3\text{-}Clpy)_2(N_3)_2$, where (3-Clpy) = 3-chloropyridine, which is known as a typical example of a spin-$\frac{1}{2}$ F–F–AF–AF tetrameric spin chain [32]. In this system, there is a gap from the singlet ground state to the triplet excited states in the absence of a magnetic field. The thermodynamic properties of the tetrameric spin chains with alternating F–F–AF–AF exchange interactions have been investigated numerically [33, 34]. The existence of a plateau at $m = 1/2$ of the saturation value has been observed. The temperature dependence of the magnetization, susceptibility and specific heat are studied to characterize the corresponding phases. In a recent paper, one of the authors considered a different tetrameric spin chain such as AF_1–F–AF_2–F [35]. By means of the numerical Lanczos method, nonlinear sigma model and bosonization approach, it has been found that a magnetization plateau appears at $\frac{1}{2}$ of the saturation value. The effects of the space modulation are reflected in the emergence of a plateau in other physical functions such as the F-dimer and the bond-dimer order parameters, and the pair-wise entanglement.

In this paper, we consider the spin-$\frac{1}{2}$ Heisenberg chains with alternating exchange supplemented by the additional modulation of the one subset of bonds with period 3, which gives the hexamer modulation of the spin exchange in the chain. Besides the very rich quantum magnetic phase diagram, this model has the ability to exhibit two new plateaus theoretically, at values 1/3 and 2/3 of the saturation. We restrict our consideration by the case where the exchange on the modulated subset of bonds is antiferromagnetic and substantially larger then the exchange on undistorted bonds. In the presence of strong magnetic field commensurate with dominant AF exchange, the model is mapped onto an effective spin-1/2 XXZ Heisenberg chain in the presence of both longitudinally uniform and spatially modulated fields. This mapping allows us to use the continuum-limit bosonization analysis and study the ground state phase diagram of the effective spin-chain model. We show that the very presence of additional modulation leads to the dynamical generation of two new energy scales in the system and to the appearance of four additional quantum phase transitions in the magnetic ground state phase diagram. These transitions manifest themselves most clearly in the presence of two new magnetization plateaus at magnetization equal to $\frac{1}{3}$ and $\frac{2}{3}$ of the saturation value. Also, the widths of the new plateaus are estimated using the scaling properties of the effective theory.

We confirm the results obtained within the continuum-limit studies of the effective model by using the exact diagonalization of finite chains and performing an accurate simulation at zero temperature using the numerical Lanczos method. There are two additional gapped phases and two corresponding magnetization plateaus in the magnetization curve of our model at values of magnetization equal to $\frac{1}{3}$ and $\frac{2}{3}$ of the saturation value. Using the numerical technique, we also study the magnetic field effects on the bond-dimer order parameter and string correlation function. Finally, treating the non-modulated weak bonds as perturbation, we obtain perfect analytical expressions for parameters characterizing the width of the two additional plateaus.

This paper is organized as follows. In section 2, we introduce our alternating space-modulated spin-1/2 model and in the strong modulated coupling limit derive an effective spin-chain Hamiltonian in section 3. In section 4, we present our analytical bosonization results. In section 5, the results of a numerical simulation are presented. Finally, we discuss and summarize our results in section 6. In the appendix, the details of calculations considering the perturbation approach used are presented.

2. The model

The Hamiltonian of the model under consideration on a periodic chain of N sites is defined as

$$\mathcal{H} = J\sum_{n=1}^{N/2}\mathbf{S}_{2n}\cdot\mathbf{S}_{2n+1} + \sum_{n=1}^{N/2}J_{\mathrm{AF}}(n)\mathbf{S}_{2n-1}\cdot\mathbf{S}_{2n} - H\sum_{n=1}^{N/2}\left(S^z_{2n-1}+S^z_{2n}\right), \tag{1}$$

where S_n is the spin-1/2 operator on the nth site, $J > 0$ and $J < 0$ denote the antiferromagnetic and ferromagnetic couplings respectively. H is the uniform magnetic field and $J_{\mathrm{AF}}(n)$ is the spatially modulated antiferromagnetic exchange. We restrict our consideration by following two types of antiferromagnetic exchange modulation corresponding to the hexameric distortion of the exchange pattern: the 'A' type:

$$J_{\mathrm{AF}}(n) = J^0_{\mathrm{AF}}\left(1+\delta\cos\left(\frac{2\pi}{3}n\right)\right), \tag{2}$$

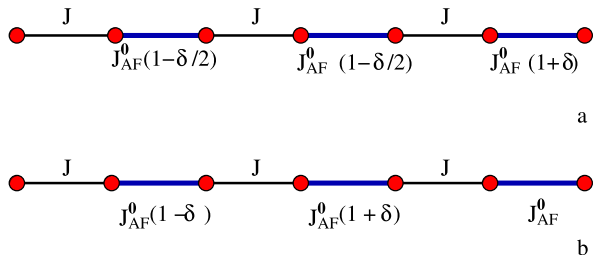

Figure 1. Schematic representation of spin chains with the hexameric modulation of spin exchange which is considered in the paper. (a) corresponds to the hexamer distortion of the exchange pattern 'A' type and (b) shows the 'B' type.

which corresponds to the hexamer modulation of the spin exchanges given in figure 1(a), and the 'B' type:

$$J_{\rm AF}(n) = J^0_{\rm AF}\left(1 - \frac{2\delta}{\sqrt{3}}\sin\left(\frac{2\pi}{3}n\right)\right), \tag{3}$$

which corresponds to the following pattern of hexamer modulation of the spin exchanges given in figure 1(b). The uniform spin-exchange coupling between spins separated by odd bonds is considered as $|J| \ll J^0_{\rm AF}$. For $\delta = 0$ and $J < 0$ the Hamiltonian equation (1) reduces to the Hamiltonian of alternating F–AF spin-1/2 chains and for $J > 0$ to the Hamiltonian of alternating AF–AF spin chains in a longitudinal uniform magnetic field.

3. The effective Hamiltonian

In the considered limiting case of strong antiferromagnetic exchange on odd bonds $J^0_{\rm AF} \gg |J|$ and for magnetic field $H \simeq J^0_{\rm AF}$, one can use the standard procedure [36, 37] to map the model equation (1) onto the effective XXZ model. The easiest way to obtain the effective model, is to start from the limit $J = 0$, where at $H = 0$ the system reduces to the set of disconnected pairs of spins in the singlet state, located on odd bonds and coupled with strong AF exchange $J_{\rm AF}(n)$. At $H \neq 0$ spins on each bond either remain in a singlet state, $|s\rangle$, with energy $E_s(n) = -0.75J_{\rm AF}(n)$ or in one of the triplet states, $|t^+\rangle$, $|t^0\rangle$ and $|t^-\rangle$ with energies $E_{t^0}(n) = 0.25J_{\rm AF}(n)$ and $E_{t^\pm}(n) = 0.25\ J_{\rm AF}(n) \mp H$, respectively. As the field H increases, the energy of the triplet state $|t^+\rangle$ decreases and at $H \simeq J_{\rm AF}(n)$ forms, together with the singlet state, a doublet of an almost degenerate low energy state, split from the remaining high energy two triplet states. This allows us to introduce the effective spin operator τ which act on these states as [36, 16]

$$\begin{aligned} \tau^z_n|s\rangle_n &= -\tfrac{1}{2}|s\rangle_n, & \tau^z_n|t^+\rangle_n &= \tfrac{1}{2}|t^+\rangle_n, \\ \tau^+_n|s\rangle_n &= |t^+\rangle_n, & \tau^+_n|t^+\rangle_n &= 0, \\ \tau^-_n|s\rangle_n &= 0, & \tau^-_n|t^+\rangle_n &= |s\rangle_n. \end{aligned} \tag{4}$$

The relation between the real spin operator $\mathbf{S}_n$ and the pseudo-spin operator τ_n in this restricted subspace can be easily derived by inspection:

$$\begin{aligned} S^\pm_{2n-1} &= -S^\pm_{2n} = \frac{1}{\sqrt{2}}\tau^\pm_n, \\ S^z_{2n-1} &= S^z_{2n} = \tfrac{1}{2}(\tfrac{1}{2} + \tau^z_n). \end{aligned} \tag{5}$$

Using equations (5), to first order and up to a constant, we easily obtain the effective Hamiltonian

$$\begin{aligned} H_{\rm eff} = \frac{J}{2}\sum_{n=1}^{N/2}\left[(\tau^x_n\tau^x_{n+1} + \tau^y_n\tau^y_{n+1}) + \frac{1}{2}\tau^z_n\tau^z_{n+1}\right] \\ - \sum_{n=1}^{N/2}[h^0_{\rm eff} + h^1_{\rm eff}(n)]\tau^z_n, \end{aligned} \tag{6}$$

where

$$h^0_{\rm eff} = H - J^0_{\rm AF} - J/4, \tag{7}$$

and

$$h^1_{\rm eff}(n) = -\delta J^0_{\rm AF}\cos(2\pi n/3) \equiv -h^{\rm A}_1\cos(2\pi n/3), \tag{8}$$

in the case of the 'A' type of modulation and

$$h^1_{\rm eff}(n) = \frac{2\delta J^0_{\rm AF}}{\sqrt{3}}\sin\left(\frac{2\pi}{3}n\right) \equiv h^{\rm B}_1\sin(2\pi n/3), \tag{9}$$

in the case of the 'B' type of modulation.

Thus, the effective Hamiltonian is nothing other than the anisotropic XXZ Heisenberg chain in an uniform and spatially trimer modulated magnetic field. The anisotropy is $\Delta = 1/2$ ($\Delta = -1/2$) in the case of a chain with antiferromagnetic (ferromagnetic) weak bonds $J > 0$ ($J < 0$). It is worth noticing that a similar problem has been studied intensively in the past few years [38–40]. At $\delta = 0$, the effective Hamiltonian reduces to the XXZ Heisenberg chain in a uniform longitudinal magnetic field. The magnetization curve of this model has only a saturation plateau corresponding to the fully polarized chain. At $H = 0$ and $J^0_{\rm AF} \gg |J|$ spins coupled by strong bonds form singlet pairs and the singlet ground state of the initial spin-chain system is well described by superposition of singlets located on strong bonds with magnetization per bond $M = 0$. In terms of the effective τ-spin model, this state corresponds to the ferromagnetic order with magnetization per site equal to its negative saturation value $m = -1/2$. In the opposite limit of very strong magnetic field $H \gg J^0_{\rm AF}$, the fully polarized state of the initial chain with magnetization per strong bond, $M = 1$, is represented in terms of an effective τ-spin chain as a fully polarized state with magnetization per site $m = 1/2$. This gives the following relation between the magnetization per strong bond of the initial spin $S = 1/2$ chain, (M), and the magnetization per site of the effective τ-chain (m): $M = m + 1/2$.

At $\delta \neq 0$, the effective model corresponds to the Heisenberg chain in spatially modulated fields with period 3. In this case, in agreement with standard theoretical predictions, additional magnetization plateaus would appear at values of magnetization $\frac{1}{3}$ and $\frac{2}{3}$ of the saturation value. Below, in this paper we use the analytical and numerical tools to analyze the magnetic phase diagram of the model under consideration and determine critical values of magnetic fields corresponding to transitions between sectors of the ground state phase diagram characterized by different magnetic behaviors.

4. Analytical results

4.1. The magnetization onset critical field H_c^- and the saturation field H_c^+

The performed mapping allows us to determine critical fields H_c^- corresponding to the onset of magnetization in the system and the saturation field H_c^+ [36]. The easiest way to get H_c^- and H_c^+ is to perform the Jordan–Wigner transformation [41] which maps the problem onto a system of interacting spinless fermions with trimerized modulated on-site potential:

$$H_{\rm sf} = \pm\frac{|J|}{2}\sum_n^{N/2}(a_n^\dagger a_{n+1} + \text{h.c.}) + \frac{|J|}{4}\sum_n^{N/2}\rho_n\rho_{n+1} - (\mu_0 + \mu_1(n))\,\rho_n, \tag{10}$$

where $\rho_n = a_n^+ a_n$, $\mu_0 = h^0_{\rm eff} - J/4 = H - J^0_{\rm AF} - J/2$, $\mu_1(n) = h^1_{\rm eff}(n)$ and the sign $+$ $(-)$ corresponds to the $J > 0$ ($J < 0$).

The lowest critical field H_c^- corresponds to that value of the chemical potential $\mu_0^{\rm c}$ for which the band of spinless fermions starts to fill up. In this limit, we can neglect the interaction term in equation (10) and obtain the model of free particles with a three-band spectrum. Below, in this section we consider only the case of the 'A' type of exchange modulation with $\mu_1(n) = h^1_{\rm eff}(n)$ given by equation (8). Generalization of this results for case 'B' is straightforward.

In this case three bands of the single-particle spectrum are given by

$$E_1(k) = -H + J^0_{\rm AF} + J\sqrt{1+\Delta^2}\cos\varphi(k), \tag{11}$$

$$E_2(k) = -H + J^0_{\rm AF} + J\sqrt{1+\Delta^2}\cos(\varphi(k) + 2\pi/3), \tag{12}$$

$$E_3(k) = -H + J^0_{\rm AF} + J\sqrt{1+\Delta^2}\cos(\varphi(k) + 4\pi/3), \tag{13}$$

where $\Delta = \delta J^0_{\rm AF}/J$

$$\varphi(k) = \frac{1}{3}\arccos\left(\frac{\cos(3k) + \Delta^3}{\sqrt{(1+\Delta^2)^3}}\right), \tag{14}$$

and $-\pi/3 < k \le \pi/3$. This gives

$$H_c^- = J^0_{\rm AF} + J\sqrt{1+\Delta^2}\cos(\varphi(\pi/3) + 4\pi/3) \quad \text{at } J > 0, \tag{15}$$

$$H_c^- = J^0_{\rm AF} - J\sqrt{1+\Delta^2}\cos\varphi(0) \qquad \text{at } J < 0. \tag{16}$$

To estimate the critical magnetic field H_c^+, which marks the transition into the phase with saturated magnetization, it is useful to make a site-dependent particle–hole transformation on the Hamiltonian of equation (10): $a_n^\dagger \to d_n$. Up to a constant the new Hamiltonian is

$$H_{\rm hole} = \mp\frac{|J|}{2}\sum_n^{N/2}(d_n^\dagger d_{n+1} + \text{h.c.}) + \frac{J}{4}\sum_n^{N/2}\rho_n^d\rho_{n+1}^d - (\mu_0^h + \mu_1(n))\rho_n^d, \tag{17}$$

where the hole chemical potential $\mu_0^h = -\mu_0 + J/2$. In terms of holes, H_c^+ corresponds to the chemical potential where the band starts to fill up, and one can neglect again the interaction term. However, the effect of the interaction is now included in the shifted value of the chemical potential for holes. After simple transformations, we obtain

$$H_c^+ = J^0_{\rm AF} + \frac{J}{2} + J\sqrt{1+\gamma^2}\cos\varphi(0) \qquad \text{at } J > 0, \tag{18}$$

$$H_c^+ = J^0_{\rm AF} + \frac{J}{2} - J\sqrt{1+\Delta^2}\cos(\varphi(\pi/3) + 4\pi/3) \quad \text{at } J < 0. \tag{19}$$

The spectrum of the system in the free fermion limit (11)–(13) allows us to determine two other important parameters which characterize the values of magnetization in the magnetization curve of the system in which the additional plateaus appear and the values of the magnetic field which correspond to the center of each plateau. Below we consider only the case $J > 0$: however, extension to the case $J < 0$ is straightforward.

At 1/3rd band-filling, all states in the lower band $E_3(k)$ are filled and separated from the empty band at $E_2(k)$ by the energy $2m_0 = E_2(k=0) - E_3(0)$. Therefore, the first magnetization plateau will appear at magnetization equal to 1/3 of the saturation value. The magnetic field at the center of the plateau is given by

$$H^0_{c1} = J^0_{\rm AF} + E_3(0) + m_0. \tag{20}$$

Analogically at 2/3rd band-filling, all states in the lower bands $E_3(k)$ and $E_2(k)$ are filled and separated from the empty band at $E_1(k)$ by the energy $2m_0 = E_1(\pi/3) - E_2(\pi/3)$. Therefore, the second magnetization plateau appears at magnetization equal to 2/3 of the saturation value and the magnetic field at the center of the plateau is given by

$$H^0_{c2} = J^0_{\rm AF} + E_2(\pi/3) + m_0. \tag{21}$$

Since at finite band-filling the effective interaction between spinless fermions cannot be ignored the width of the plateau differs from its bare value $2m_0$. In section 4.2 we use the continuum-limit bosonization treatment of the effective spin-chain model equation (10) to determine parameters characterizing the appearance and scale of the magnetization plateaus.

4.2. Magnetization plateaus: $H^\pm_{c_1}$ and $H^\pm_{c_2}$

To determine parameters characterizing the appearance and scale of the magnetization plateaus, we use the continuum-limit bosonization treatment of the model equation (6). Following the usual procedure in the low energy limit, we bosonize the spin degrees of freedom at fixed magnetization m and the interaction term becomes [42]

$$\tau_n^z = m + \sqrt{\frac{K}{\pi}}\,\partial_x\phi(x) + \frac{A_1}{\pi}\sin(\sqrt{4\pi K}\phi(x) + (2m+1)\pi n), \tag{22}$$

$$\tau_n^+ = \mathrm{e}^{-\mathrm{i}\sqrt{\pi/K}\theta(x)} \times\left[1 + \frac{B_1}{\pi}\sin(\sqrt{4\pi K}\phi(x) + (2m+1)\pi n)\right], \tag{23}$$

where A_1 and B_1 are non-universal real constants of the order of unity [43] and m is the magnetization (per site) of the chain. Here $\phi(x)$ and $\theta(x)$ are dual bosonic fields, $\partial_t\phi = v_s\partial_x\theta$, and satisfy the following commutation relations:

$$[\phi(x), \theta(y)] = \mathrm{i}\Theta(y-x), \qquad [\phi(x), \theta(x)] = \mathrm{i}/2, \quad (24)$$

and $K(\Delta, m)$ is the spin stiffness parameter for a chain with anisotropy Δ and magnetization m. At zero magnetization

$$K(\Delta, 0) = \frac{\pi}{2(1-\arccos\Delta)}. \quad (25)$$

Therefore, at $m = 0$, $K = 0.75$ for $J > 0$ and $K = 1.5$ for $J < 0$. At the transition line into the ferromagnetic phase, where the magnetization reaches its saturation value $m_{\mathrm{sat}} = 0.5$, the spin stiffness parameter takes the universal value $K(\Delta, 0.5) = 1$ [44]. Respectively for finite magnetization, at $0 < m < m_{\mathrm{sat}}$ and $J > 0$, the function $K(\Delta, m)$ monotonically increases with enhancing m and reaches its maximum value at saturation magnetization, $K(\Delta, m_{\mathrm{sat}}) = 1$, while for $J < 0$, it monotonically decreases with increasing m and reaches its minimum value at saturation magnetization $K(\Delta, 0.5) = 1$.

Using (22) and (23), in the case of the 'A' type of exchange modulation, we get the following bosonized Hamiltonian:

$$H^{\mathrm{A}}_{\mathrm{Bos}} = \int \mathrm{d}x \left\{ \frac{v_s}{2}[(\partial_x\phi)^2 + (\partial_x\theta)^2] - h^0_{\mathrm{eff}}\sqrt{\frac{K}{\pi}}\partial_x\phi + \frac{h^{\mathrm{A}}_1}{2\pi a_0}\left[\sin\left(2\pi\left(m+\frac{1}{6}\right)n + \sqrt{4\pi K}\phi\right) + \sin(2\pi(m+\tfrac{5}{6})n + \sqrt{4\pi K}\phi)\right]\right\}, \quad (26)$$

while in the case of the 'B' type of modulation—following

$$H^{\mathrm{B}}_{\mathrm{Bos}} = \int \mathrm{d}x \left\{ \frac{v_s}{2}[(\partial_x\phi)^2 + (\partial_x\theta)^2] - h^0_{\mathrm{eff}}\sqrt{\frac{K}{\pi}}\partial_x\phi + \frac{h^{\mathrm{B}}_1}{2\pi a_0}\left[\cos\left(2\pi\left(m+\frac{1}{6}\right)n + \sqrt{4\pi K}\phi\right) - \cos(2\pi(m+\tfrac{5}{6})n + \sqrt{4\pi K}\phi)\right]\right\}. \quad (27)$$

From the bosonized Hamiltonian, one easily gets the commensurate values of magnetization $m = \pm 1/6$ where a magnetization plateau appears. Away from this commensurate value of magnetization, arguments of cosine terms are strongly oscillating and in the continuum limit their contribution is irrelevant. Therefore in this case, the model is described by the effective Gaussian model, indicating a gapless character of excitations and continuously increasing magnetization of the chain with increasing magnetic field.

At commensurate values of magnetization $m = \pm 1/6$, the cosine term in (26) and (27) is not oscillating and therefore the modulated magnetic field term comes into play. Up to an irrelevant shift on a constant of the bosonic field, the generalized Hamiltonian which describes the system at commensurate magnetization is given by

$$H^i_{\mathrm{Bos}} = \int \mathrm{d}x \left\{ \frac{v_s}{2}[(\partial_x\phi)^2 + (\partial_x\theta)^2] + \frac{m^i_0}{2\pi a_0}\cos(\sqrt{4\pi K}\phi) - h_0\sqrt{\frac{K}{\pi}}\partial_x\phi \right\} \qquad i = \mathrm{A}, \mathrm{B}. \quad (28)$$

where

$$m^{\mathrm{A}}_0 = \delta J^0_{\mathrm{AF}} \qquad \text{and} \qquad m^{\mathrm{B}}_0 = 2m^{\mathrm{A}}_0/\sqrt{3}. \quad (29)$$

The Hamiltonian (28) is the standard Hamiltonian for the commensurate–incommensurate transition which has been intensively studied in the past using bosonization [45] and the Bethe ansatz [46]. Below, we use these results to describe the magnetization plateau and the transitions from a gapped (plateau) to gapless paramagnetic phases.

Let us first consider $h^0_{\mathrm{eff}} = 0$. In this case, the continuum theory of the initial hexamer spin-chain model in the magnetic field $H = J^0_{\mathrm{AF}} + J/4$ is given by the quantum sine–Gordon (SG) model with a massive term $\sim h^i_1\cos(\sqrt{4\pi K}\phi)$. From the exact solution of the SG model [47], it is known that the excitation spectrum is gapless for $K \geq 2$ and has a gap in the interval $0 < K < 2$. The exact relation between the soliton mass M and the bare mass m_0 is given by [48]

$$M = J\mathcal{C}(K)\,(m_0/J)^{1/(2-K)}, \quad (30)$$

where

$$\mathcal{C}(K) = \frac{2}{\sqrt{\pi}}\frac{\Gamma(\frac{K}{8-2K})}{\Gamma(\frac{2}{4-K})}\left[\frac{\Gamma(1-K/4)}{2\Gamma(K/4)}\right]^{2/(4-K)}. \quad (31)$$

Here Γ is the Gamma function and the spin stiffness parameter K depends on the sign of J and magnetization m.

In the gapped phase, the ground state properties of the system are determined by the dominant potential energy term $\sim\cos(\sqrt{4\pi K}\phi)$ and therefore, in the gapped phases, the field ϕ is pinned in one of the vacua:

$$\langle 0|\sqrt{4\pi K}\phi|0\rangle = (2n+1)\pi, \quad (32)$$

to ensure the minimum of the energy.

At $h^0_{\mathrm{eff}} \neq 0$ (i.e. $H \neq J^0_{\mathrm{AF}} + J/4$), the presence of the gradient term in the Hamiltonian equation (28) makes it necessary to consider the ground state of the sine–Gordon model in sectors with nonzero topological charge. The effective chemical potential $\sim h^0_{\mathrm{eff}}\sqrt{\frac{K}{\pi}}\partial_x\phi$ tends to change the number of particles in the ground state, i.e. to create a finite and uniform density of solitons. It is clear that the gradient term in (28) can be eliminated by a gauge transformation $\phi \to \phi + h^0_{\mathrm{eff}}\sqrt{\frac{K}{\pi}}\,x$. However, this immediately implies that the vacuum distribution of the field ϕ will be shifted with respect to the minima (32). This competition between contributions of the smooth and modulated components of the magnetic field is resolved as a continuous phase transition from a gapped state at $|h^0_{\mathrm{eff}}| < M$ to a gapless (paramagnetic) phase at $|h^0_{\mathrm{eff}}| > M$, where M is the soliton mass [45]. This condition gives two critical values of the magnetic field for each plateau $H^{\pm}_{\mathrm{c},j} = H^0_{\mathrm{c},j} \pm M_j$.

In the case of a chain with AF exchange on weak bonds ($J > 0$) this gives

$$H^{\pm}_{c,1} = J^0_{AF} \pm J\mathcal{C}(K_1)\,(c_i\gamma)^{1/(2-K_1)}, \tag{33}$$

$$H^{\pm}_{c,2} = J^0_{AF} + J \pm J\mathcal{C}(K_2)\,(c_i\gamma)^{1/(2-K_2)}, \quad i = \mathrm{A, B} \tag{34}$$

where

$$K_1 = K(1/2, -1/6), \quad \text{and} \quad K_2 = K(1/2, +1/6), \quad \text{and} \quad c_A = 1, c_B = 2/\sqrt{3}. \tag{35}$$

Respectively, in the case of a chain with ferromagnetic exchange on weak bonds ($J < 0$) we obtain

$$H^{\pm}_{c,1} = J^0_{AF} + J \pm |J|\mathcal{C}(K_1')\,(c_i\gamma)^{1/(2-K_1')}, \tag{36}$$

$$H^{\pm}_{c,2} = J^0_{AF} \pm |J|C(K_2')\,(c_i\gamma)^{1/(2-K_2')}, \qquad i = \mathrm{A, B} \tag{37}$$

where

$$K_1' = K(-1/2, -1/6) \quad \text{and} \quad K_2' = K(-1/2, +1/6). \tag{38}$$

Correspondingly the width of each magnetization plateau is given by

$$H^{+}_{c,j} - H^{-}_{c,j} = 2M_j = \begin{cases} 2J\mathcal{C}(K_j)\,(m_0^j/J)^{1/(2-K_j)} & \text{at } J > 0 \\ 2|J|\mathcal{C}(K_j')\,(m_0^j/|J|)^{1/(2-K_j')} & \text{at } J < 0 \end{cases} \qquad j = 1, 2. \tag{39}$$

To estimate the numerical value of the spin stiffness parameter K at magnetization m and anisotropy Δ we use the following *ansatz*:

$$K(\Delta, m) = K(\Delta, 0) + \frac{|m|}{m_{sat}}(1 - K(\Delta, 0)). \tag{40}$$

Here, we assume that with increasing magnetization, the spin stiffness parameter *monotonically reaches its extremum* $K = 1$ *at* $m = m_{sat}$. This ansatz gives that $K_1 = K_2 \simeq 0.87$ for $J > 0$ and $K_1 = K_2 \simeq 1.335$ for $J < 0$. It is straightforward to get that, in the antiferromagnetic case, the width of the magnetization plateau scales as $\delta^{1.13}$ while in the case of a chain with ferromagnetic weak bonds it scales as $\delta^{1.50}$.

In order to investigate the detailed behavior of the ground state magnetic phase diagram and to test the validity of the picture obtained from the continuum-limit bosonization treatment, below in this paper we present results of numerical calculations using the Lanczos method of exact diagonalization for finite chains.

5. Numerical simulation

A very famous and accurate method in the field of numerical simulation is known as the Lanczos method. In order to explore the nature of the spectrum and the phase transition, we use the Lanczos method to diagonalize numerically the model (1) with periodic boundary conditions.

In this section, to find the effect of a magnetic field on the ground state phase diagram of the model, we calculate the spin gap, the magnetization, the string correlation function and the bond-dimer order parameter for finite chains with lengths $N = 12$, 18 and 24 and periodic boundary conditions.

Since in a critical field, the energy gap should be closed, the best way to find the critical fields is the investigation of the energy gap, which is recognized as the difference between the energies of the first excited state and the ground state in finite chains. In figure 2, we have presented results of these calculations on the energy gap for the exchange parameter corresponding to the 'A' and 'B' types as

$$J^0_{AF} = \tfrac{19}{3}, \quad \delta = \tfrac{2}{19}, \quad J = -1, \tag{41a}$$

$$J^0_{AF} = \tfrac{19}{3}, \quad \delta = \tfrac{2}{19}, \quad J = +1, \tag{41b}$$

$$J^0_{AF} = 6, \quad \delta = \tfrac{1}{6}, \quad J = -1, \tag{41c}$$

$$J^0_{AF} = 6, \quad \delta = \tfrac{1}{6}, \quad J = +1. \tag{41d}$$

and chain lengths $N = 12$, 18 and 24. At $H = 0$, it is clearly seen that the spectrum of the model is gapped. As soon as the magnetic field applies, the energy gap decreases linearly with H and vanishes at H^-_c. This is the first level crossing between the ground state energy and the first excited state energy. By further increasing the magnetic field, three gapless regions:

$$H^-_c < H < H^-_{c_1}, \quad H^+_{c_1} < H < H^-_{c_2}, \quad H^+_{c_2} < H < H^+_c, \tag{42}$$

and three gapped regions:

$$H^-_{c_1} < H < H^+_{c_1}, \quad H^-_{c_2} < H < H^+_{c_2}, \quad H > H^+_c. \tag{43}$$

are seen in figure 2. Oscillations of the energy gap in gapless regions are the result of level crossings in finite size systems. One should note that the energy gap in the last gapped region, $H > H^+_c$, growths linearly with the magnetic field H which is an indication of the saturated ferromagnetic phase. Therefore with respect to the non-modulated case $\delta = 0$ [16], two new gapped regions are created by adding δ. To find the critical fields, we have used the phenomenological renormalization group (PRG) method [16]. As an example, critical fields for the exchanges $J^0_{AF} = \frac{19}{3}$, $\delta = \frac{2}{19}$ and $J = -1$ are given as follows:

$$H^-_c = 5.67 \pm 0.01, \quad H^+_c = 6.65 \pm 0.01, \quad H^-_{c_1} = 5.75 \pm 0.01, \quad H^+_{c_1} = 5.91 \pm 0.01, \quad H^-_{c_2} = 6.00 \pm 0.01, \quad H^+_{c_2} = 6.62 \pm 0.01. \tag{44}$$

The first insight into the magnetic order of the ground state of the system is determined by studying the magnetization process. The magnetization along the field axis is defined as

$$M^z = \frac{1}{N}\sum_{n=1}^{N}\langle Gs|S^z_n|Gs\rangle, \tag{45}$$

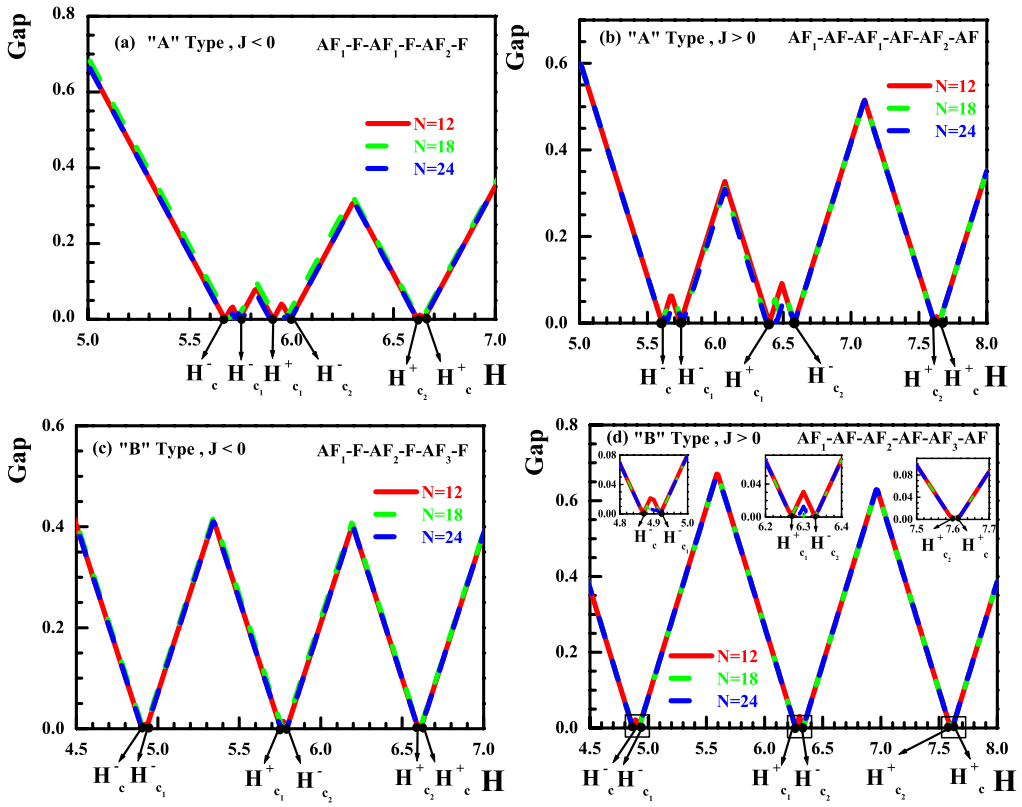

Figure 2. Difference between the energy of the first lowest level and the ground state (Gap) as a function of the magnetic field, H for chains with exchanges (a) $J^0_{\rm AF} = \frac{19}{3}$, $\delta = \frac{2}{19}$ and $J = -1$, (b) $J^0_{\rm AF} = \frac{19}{3}$, $\delta = \frac{2}{19}$ and $J = 1$, (c) $J^0_{\rm AF} = 6$, $\delta = \frac{1}{6}$ and $J = -1$, and (d) $J^0_{\rm AF} = 6$, $\delta = \frac{1}{6}$ and $J = 1$, and lengths $N = 12$, 18 and 24.

where the notation $\langle Gs| \cdot |Gs\rangle$ represents the ground state expectation value. In figure 3, we have plotted the magnetization along the applied magnetic field, M^z, versus H for chain lengths $N = 12$, 18 and 24 and different exchange parameters corresponding to the 'A' and 'B' types. As it is clearly seen, in the absence of the magnetic field $H = 0$, the magnetization is zero. By increasing the magnetic field, the magnetization remains zero up to the first critical field $H = H^-_{\rm c}$. This part of the magnetization is known as the zero plateau. This behavior is in agreement with expectation based on the general statement that, in the gapped phases, the magnetization along the applied field appears only at a finite critical value of the magnetic field equal to the spin gap. Besides the standard zero and saturation plateaus at $H < H^-_{\rm c}$ and $H > H^+_{\rm c}$, respectively, two additional plateaus are seen at $M^z = \frac{1}{3}M_{\rm sat}$ and $M^z = \frac{2}{3}M_{\rm sat}$, where both of them satisfy the Oshikawa–Yamanaka–Affleck (OYA) condition. To check that the middle plateaus are not a finite size effect, we performed the size scaling [49] of their width and found that the size of the plateaus interpolates to a finite value when $N \longrightarrow \infty$. As has been clearly seen in figures 2 and 3, the width of plateaus and the mentioned gapped regions grow by increasing the modulation δ. In the insets of figure 3, the magnetization on site, $M^z_n = \langle Gs|S^z_n|Gs\rangle$, as a function of the site number n is plotted for some values of the magnetic field corresponding to the plateaus at $\frac{1}{3}M_{\rm sat}$ and $\frac{2}{3}M_{\rm sat}$ and length $N = 24$. As we observe, the system shows a well-pronounced modulation of the on-site magnetization, where magnetization on weak modulated bonds is larger than on strong modulated bonds. This distribution remains almost unchanged within the plateau at $\frac{1}{3}M_{\rm sat}$ for $H^-_{\rm c_1} < H < H^-_{\rm c_1}$ and the plateau at $\frac{2}{3}M_{\rm sat}$ for fields $H^-_{\rm c_2} < H < H^+_{\rm c_2}$.

By analyzing the results on the energy gap, we found that the spectrum is gapped in the absence of the magnetic field which is one of the properties of the Haldane phase. Since we have considered the very strong antiferromagnetic (AF) exchange on odd bonds, the Haldane phase cannot be found and it is expected to be the gapped dimer phase. This phase can be recognized from studying the string correlation function. The string correlation function in a chain of length N, defined only for odd l, is [50]

$$O_{\rm Str}(l, N) = -\left\langle \exp\left\{ i\pi \sum_{2n+1}^{2n+l+1} S^x_k \right\} \right\rangle. \qquad (46)$$

In particular, we calculated the string correlation function for different finite chain lengths $N = 12$, 18 and 24. Since the model has the $U(1)$ symmetry in the presence of a magnetic field, we consider the transverse component of the string correlation function. Figure 4 presents the Lanczos results on the string correlation function for the chain with lengths $N = 12$, 18 and 24 and different exchange parameters corresponding to the 'A' and 'B' types. As can be seen from this figure, at $H < H^-_{\rm c}$, the string correlation function $O_{\rm Str}(l, N)$ is saturated and the hexamer chain system is in the dimer phase. As soon as the magnetic field increases from the

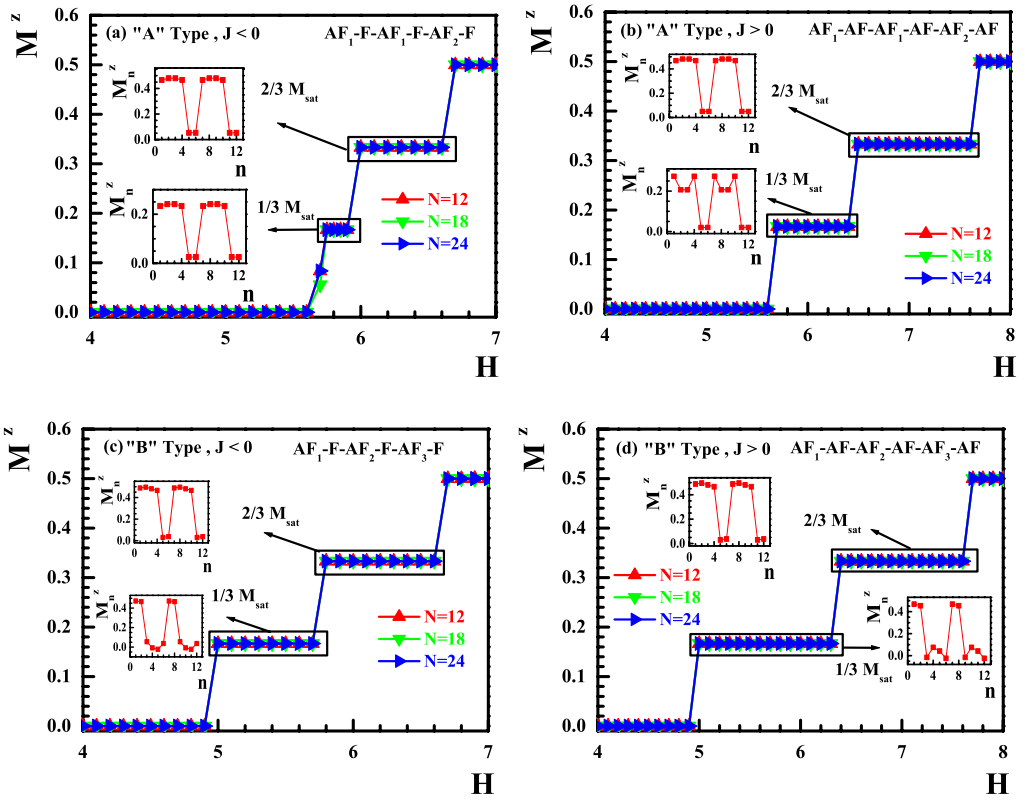

Figure 3. Magnetization as a function of the magnetic field, H for chains with exchanges (a) $J^0_{\rm AF} = \frac{19}{3}$, $\delta = \frac{2}{19}$ and $J = -1$, (b) $J^0_{\rm AF} = \frac{19}{3}$, $\delta = \frac{2}{19}$ and $J = 1$, (c) $J^0_{\rm AF} = 6$, $\delta = \frac{1}{6}$ and $J = -1$, and (d) $J^0_{\rm AF} = 6$, $\delta = \frac{1}{6}$ and $J = 1$, and lengths $N = 12$, 18 and 24. In the insets, the magnetization on site as a function of the site number n is plotted for a value of the magnetic field in the region of the plateau of $1/3M_{\rm sat}$ and $2/3M_{\rm sat}$ for length $N = 24$.

first critical field, as expected the string correlation function decreases very rapidly and reaches zero in the thermodynamic limit, which shows that only the dimer phase remains stable in the presence of a magnetic field less than $H_{\rm c}^-$. The nonzero values of the string correlation function in the region $H > H_{\rm c}^-$ are finite size effects and it is completely clear that in the thermodynamic limit $N \longrightarrow \infty$ will be zero.

An additional insight into the nature of different phases can be obtained by studying the correlation functions. Since there are three kinds of space-modulated exchanges in our hexameric chain model, we define the following bond-dimer order parameters:

$$
\begin{aligned}
d_r^{\rm AF_1} &= \frac{6}{N}\sum_{n=0}^{(N/6)-1}\langle Gs|\mathbf{S}_{6n+1}\cdot\mathbf{S}_{6n+2}|Gs\rangle,\\
d_r^{\rm AF_2} &= \frac{6}{N}\sum_{n=0}^{(N/6)-1}\langle Gs|\mathbf{S}_{6n+3}\cdot\mathbf{S}_{6n+4}|Gs\rangle,\\
d_r^{\rm AF_3} &= \frac{6}{N}\sum_{n=0}^{(N/6)-1}\langle Gs|\mathbf{S}_{6n+5}\cdot\mathbf{S}_{6n+6}|Gs\rangle,
\end{aligned}
\qquad (47)
$$

where summations are taken over the space-modulated antiferromagnetic bonds. In figure 5, we have plotted $d_r^{\rm AF_1}$, $d_r^{\rm AF_2}$ and $d_r^{\rm AF_3}$ versus magnetic field H for chains of length $N = 24$ with different exchange parameters corresponding to the 'A' and 'B' types. As is seen from this figure, at $H < H_{\rm c}^-$ spins on all antiferromagnetic space-modulated bonds are in a singlet state $d_r^{\rm AF_1} = d_r^{\rm AF_2} = d_r^{\rm AF_3} \simeq -0.75$, while at $H > H_{\rm c}^+$, the bond-dimer order parameter d_r, is equal to the saturation value $d_r^{\rm AF_1} = d_r^{\rm AF_2} = d_r^{\rm AF_3} \sim 0.25$ and the ferromagnetic long-range order along the magnetic field axis is present. However, in the considered case of strong antiferromagnetic exchanges ($J^0_{\rm AF} \gg |J|$) and high critical fields, quantum fluctuations are substantially suppressed and calculated averages of spin correlations are very close to their nominal values.

For intermediate values of the magnetic field, at $H_{\rm c}^- < H < H_{\rm c}^+$ the data presented in figure 5 gives us a possibility to trace the mechanism of singlet-pair melting with increasing the magnetic field. As follows from figure 5, at values of the magnetic field slightly above $H_{\rm c}^-$ spin singlet pairs start to melt in all modulated bonds simultaneously and almost with the same intensity. By further increasing of H and for fields $H > H_{\rm c}^-$, melting of weak modulated bonds gets more intensive. However, at $H = H_{\rm c_1}^-$ the process of melting stops and the bond-dimer order parameter remains constant up to the critical field $H = H_{\rm c_1}^+$. As is seen in figures 5(a) and (b) for the 'A' type of modulation, in the 1/3-plateau state, weak and strong modulated bonds manifest on-site singlet features with dimerization values $\simeq -0.25$ and $\simeq -0.70$, respectively. In contrast, for the 'B' type of modulation (figures 5(c) and (d)), weak modulated bonds are almost polarized with dimerization value $\simeq 0.18$, while intermediate and strong bonds manifest strong on-site singlet features with value

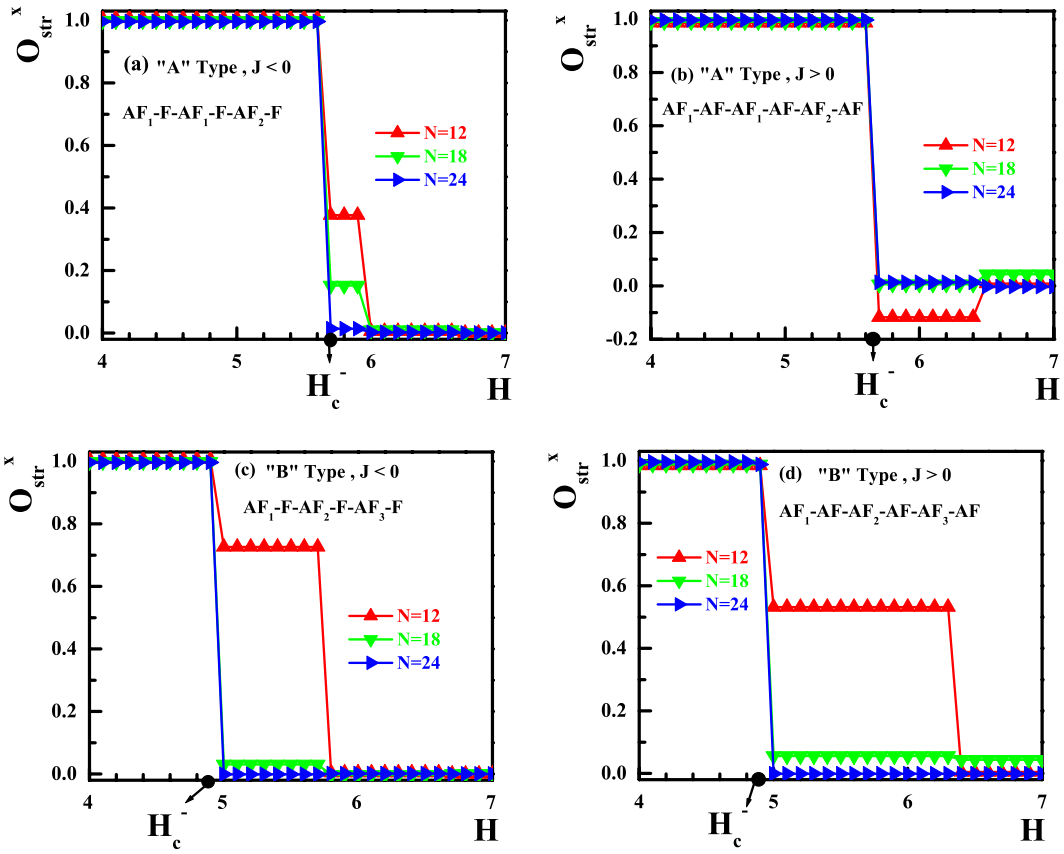

Figure 4. String correlation function as a function of the magnetic field, H for chains with exchanges (a) $J^0_{\rm AF} = \frac{19}{3}$, $\delta = \frac{2}{19}$ and $J = -1$, (b) $J^0_{\rm AF} = \frac{19}{3}$, $\delta = \frac{2}{19}$ and $J = 1$, (c) $J^0_{\rm AF} = 6$, $\delta = \frac{1}{6}$ and $J = -1$, and (d) $J^0_{\rm AF} = 6$, $\delta = \frac{1}{6}$ and $J = 1$, and lengths $N = 12$, 18 and 24.

$\simeq -0.70$. By increasing the magnetic field more and for fields $H > H^+_{c_1}$, the melting of the weak bonds happens intensively and at $H = H^-_{c_2}$ the process of melting stops and remains stable up to the critical field $H^+_{c_2}$. It is clearly seen, in the 2/3-plateau state, that weak bonds for 'A' type and weak and intermediate modulated bonds for 'B' type are polarized ($\simeq 0.22$), but strong bonds still manifest strong on-site singlet features ($\simeq -0.65$). Finally, for $H^+_{c_2}$ strong bonds start to melt more intensively while the polarization of weak bonds increases slowly and at $H = H^+_{\rm c}$ all weak and strong bonds achieve an identical, almost fully polarized state.

6. Conclusion

In this paper, we have studied the effect of additional modulation of strong antiferromagnetic bonds on the ground state magnetic phase diagram of the 1D spin-1/2 chain with alternating exchange. In particular, we focus our studies on the chain with hexamer modulation, where the spin exchange on even bonds is the same, while the strong antiferromagnetic exchange on odd bonds is modulated with period 3.

In the limit where the odd couplings are dominant, we mapped the model to an effective XXZ Heisenberg chain with anisotropy Δ in an effective uniform and spatially trimer modulated magnetic field. The anisotropy parameter is $\Delta = \frac{1}{2}$ in the case of antiferromagnetic exchange on even bonds and $\Delta = -\frac{1}{2}$ in the case of ferromagnetic exchange on even bonds. Using the continuum-limit bosonization treatment of the effective spin-chain model, we have shown that the additional modulation of the strong bonds with period 3 and amplitude $\simeq \delta$ leads to the generation of two gaps in the excitation spectrum of the system at magnetization equal to 1/3 and 2/3 of its saturation value. As a result of this new energy scale formation, the magnetization curve of the system $M(H)$ exhibits two plateaus at $M = \frac{1}{3}M_{\rm sat}$ and $M = \frac{2}{3}M_{\rm sat}$. The width of the plateaus is proportional to the excitation gap and scales as δ^ν, where the critical exponent $\nu = 1.13 \pm 0.01$ in the case of an AF exchange on even bonds and $\nu = 1.50 \pm 0.01$ in the case of ferromagnetic exchange on even bonds.

For a complete description of the model, we supplement our analysis by a very accurate numerical simulation. Using the Lanczos method of numerical diagonalizations for chains up to $N = 24$, we have studied the effects of an external magnetic field on the ground state properties of the system. In the first part of the numerical experiment, we have focused on the energy gap of the system. Our results showed that, with respect to the non-modulated chain, two new gapped regions were created by adding the modulation. The widths of the mentioned gapped regions grow by increasing the parameter of modulation δ. In the second part of the numerical experiment, we have studied the magnetization process. We provided a clear picture of the magnetization which showed that two magnetization plateaus appear at values $\frac{1}{3}M_{\rm sat}$ and

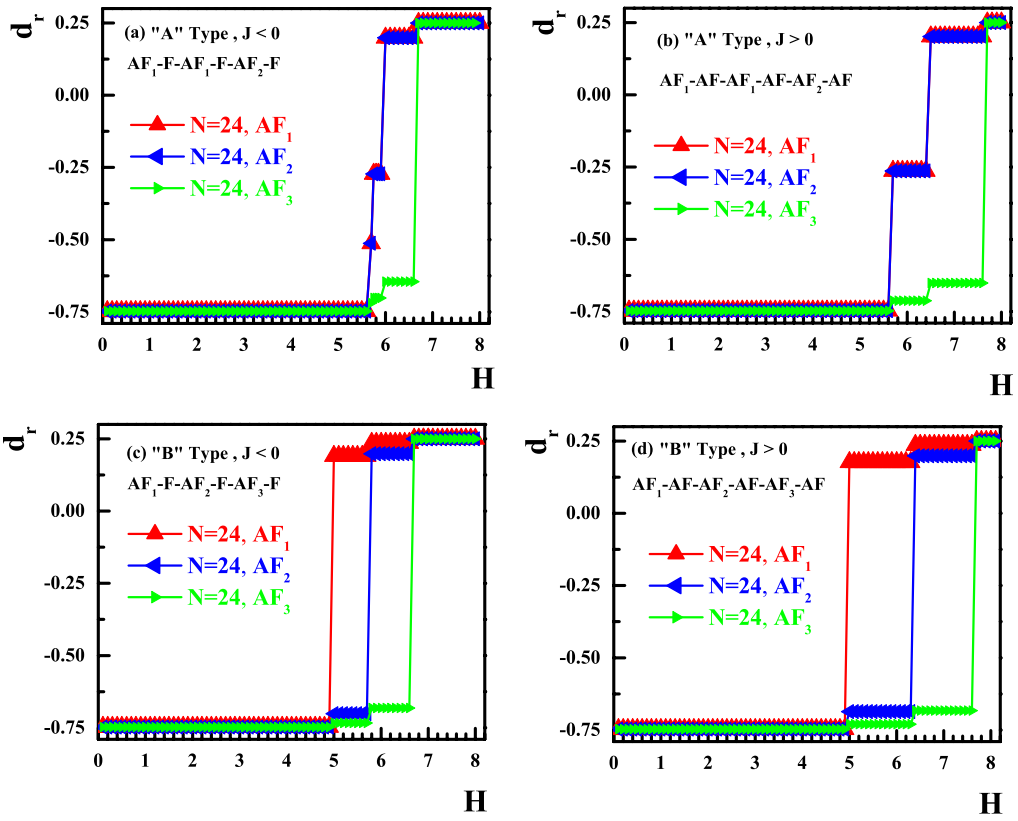

Figure 5. The bond-dimer order parameter as a function of the magnetic field, H for chains with exchanges (a) $J^0_{\rm AF} = \frac{19}{3}$, $\delta = \frac{2}{19}$ and $J = -1$, (b) $J^0_{\rm AF} = \frac{19}{3}$, $\delta = \frac{2}{19}$ and $J = 1$, (c) $J^0_{\rm AF} = 6$, $\delta = \frac{1}{6}$ and $J = -1$, and (d) $J^0_{\rm AF} = 6$, $\delta = \frac{1}{6}$ and $J = 1$, and length $N = 24$.

$\frac{2}{3}M_{\rm sat}$ in the new gapped regions. To find additional insight into the nature of the different phases, we also calculated the on-site magnetization, the string correlation function and the bond-dimer order parameters. The on-site magnetization showed a microscopic picture of the direction of spins on different sites, when the system is in the new gapped regions. On the other hand, by studying the string correlation function, we found that in the absence of the magnetic field, the suggested alternating chain is in the dimer phase and this phase remains stable in the presence of an external magnetic field up to the first critical field. Finally, we studied the effect of the magnetic field on the ground state phase diagram of the model by means of the perturbation approach. Using perturbation theory, we provided the analytical results for the critical fields that these results were in good agreement with the obtained numerical experiment results.

Acknowledgments

We wish to thank N Avalishvili for a helpful communication. GIJ acknowledges support from the SCOPES grant IZ73Z0-128058 and the Georgian NSF grant no. ST09/4-447.

Appendix . Perturbation results

In this section, we study the effect of the magnetic field on the ground state phase diagram of the model, using the perturbation approach. We try to find the analytical results for the critical fields. The behavior of the model (1) in the limit of strong couplings on the odd bonds $J_{\rm AF}(n) \gg J$ is interesting. For this aim, it is convenient to rewrite the Hamiltonian equation (1) in the form

$$\begin{aligned} \mathcal{H} &= \mathcal{H}_0 + \mathcal{V} \\ \mathcal{H}_0 &= \sum_{n=1}^{N/2} J_{\rm AF}(n)\mathbf{S}_{2n-1}\cdot\mathbf{S}_{2n} - h\sum_{n=1}^{N} S^z_n \\ \mathcal{V} &= J\sum_{n=1}^{N/2}\mathbf{S}_{2n}\cdot\mathbf{S}_{2n+1}. \end{aligned} \tag{48}$$

The unperturbed part, $\mathcal{H}_0$, is the Hamiltonian of $N/2$ non-interacting pairs of spins. The eigenstate of the unperturbed Hamiltonian is written as a product of pair states. By solving the eigenvalue equation of an individual pair, one can easily find the eigenstates as mentioned in section 3. Let us start with the case of $\delta = 0$. Since the ground state energy of a distinct pair is twofold-degenerate at $H = J_{\rm AF}(n)$, the ground state energy of the unperturbed Hamiltonian $\mathcal{H}_0$ is $2^{N/2}$ times degenerate [36]. The perturbation $\mathcal{V}$ splits this degeneracy. By applying the first-order and second-order perturbation theory for finite chains with periodic boundary conditions and generalizing results to the thermodynamic limit, one can find two critical fields. In the case modulated chain, $\delta \neq 0$, there are different kinds of bonds: strong and weak. In this case, by increasing the magnetic field, first weak

Table A.1. The critical fields which are obtained by the perturbation theory and the corresponding values obtained by the numerical experiment in the hexameric chain of the 'A' type and $J < 0$, the 'A' type and $J > 0$, the 'B' type and $J < 0$ and the 'B' type and $J > 0$.

Critical fields	Perturbation results	Numerical results
	'A' type and $J < 0$	
H_c^-	5.62	5.67 ± 0.01
$H_{c_1}^-$	5.75	5.75 ± 0.01
$H_{c_1}^+$	5.87	5.91 ± 0.01
$H_{c_2}^-$	6.00	6.00 ± 0.01
$H_{c_2}^+$	6.62	6.62 ± 0.01
H_c^+	6.62	6.65 ± 0.01
	'A' type and $J > 0$	
H_c^-	5.62	5.61 ± 0.01
$H_{c_1}^-$	5.75	5.75 ± 0.01
$H_{c_1}^+$	6.37	6.40 ± 0.01
$H_{c_2}^-$	6.50	6.59 ± 0.01
$H_{c_2}^+$	7.62	7.61 ± 0.01
H_c^+	7.62	7.66 ± 0.01
	'B' type and $J < 0$	
H_c^-	4.90	4.90 ± 0.01
$H_{c_1}^-$	4.90	4.96 ± 0.01
$H_{c_1}^+$	5.75	5.75 ± 0.01
$H_{c_2}^-$	5.75	5.78 ± 0.01
$H_{c_2}^+$	6.59	6.60 ± 0.01
H_c^+	6.59	6.61 ± 0.01
	'B' type and $J > 0$	
H_c^-	4.90	4.87 ± 0.01
$H_{c_1}^-$	4.90	4.92 ± 0.01
$H_{c_1}^+$	6.25	6.27 ± 0.01
$H_{c_2}^-$	6.25	6.33 ± 0.01
$H_{c_2}^+$	7.59	7.60 ± 0.01
H_c^+	7.59	7.61 ± 0.01

bonds melt and go to the triplet state with respect to the strong bonds. Therefore, it is natural to find four additional critical fields with respect to the non-modulated case, $\delta = 0$.

The determined critical fields for a hexameric chain of the 'A' type with $J < 0$ and by using the perturbation approach are

$$\begin{aligned} H_c^- &= J_{AF}^0\left(1-\frac{\delta}{2}\right)+\frac{J}{4}-\frac{J^2}{12\delta J_{AF}^0}, \\ H_{c_1}^- &= J_{AF}^0\left(1-\frac{\delta}{2}\right)+\frac{J}{4}, \\ H_{c_1}^+ &= J_{AF}^0\left(1-\frac{\delta}{2}\right)-\frac{J^2}{12\delta J_{AF}^0}, \\ H_{c_2}^- &= J_{AF}^0\left(1-\frac{\delta}{2}\right), \\ H_{c_2}^+ &= J_{AF}^0\left(1+\frac{\delta}{2}\right)+\frac{J}{4}+\frac{J^2}{12\delta J_{AF}^0}, \\ H_c^+ &= J_{AF}^0\left(1+\frac{\delta}{2}\right)+\frac{J}{4}+\frac{J^2}{12\delta J_{AF}^0}. \end{aligned} \tag{49}$$

Generalization of this result for 'A' type and $J > 0$, 'B' type and $J < 0$ and 'B' type and $J > 0$ is straightforward. In table A.1, the numerical and perturbation analytical results of critical fields were compared for a chain of the 'A' type and $J < 0$, the 'A' type and $J > 0$, the 'B' type and $J < 0$ and the 'B' type and $J > 0$. The accuracy of analytical results are to two significant digits. We emphasize that the perturbation results are in good agreement with the obtained numerical experiment results.

References

[1] Haldane F D M 1983 *Phys. Rev. Lett.* **50** 1153
[2] Oshikawa M, Yamanaka M and Affleck I 1997 *Phys. Rev. Lett.* **78** 1984
[3] Takada S 1992 *J. Phys. Soc. Japan* **61** 428
[4] Hida K and Takada S 1992 *J. Phys. Soc. Japan* **61** 1879
[5] Hida K 1992 *Phys. Rev.* B **46** 8268
[6] Kohmoto M and Tasaki H 1992 *Phys. Rev.* B **46** 3486
[7] Hida K 1993 *J. Phys. Soc. Japan* **62** 439
[8] Yamanaka M, Hatsugai Y and Kohmoto M 1993 *Phys. Rev.* B **48** 9555
[9] Hida K 1994 *J. Phys. Soc. Japan* **63** 2514
[10] Sakai T 1995 *J. Phys. Soc. Japan* **64** 251
[11] Uhrig G S and Schulz H J 1996 *Phys. Rev.* B **54** R9624
[12] Barnes T, Riera J and Tennant D A 1999 *Phys. Rev.* B **59** 11384
[13] Bocquet M and Jolicoeur Th 2000 *Eur. Phys. J.* B **14** 47
[14] Yamamoto S and Funase K 2005 *Low Temp. Phys.* **31** 740
[15] Zheng W, Hamer C J and Singh R R P 2006 *Phys. Rev.* B **74** 172407
[16] Mahdavifar S and Akbari A 2008 *J. Phys. Soc. Japan* **77** 024710
[17] Abouie J and Mahdavifar S 2008 *Phys. Rev.* B **78** 184437
[18] Hagiwara M, Narumi Y, Kindo K, Kobayashi T C, Yamakage H, Amaya K and Schumauch G 1997 *J. Phys. Soc. Japan* **66** 1792
[19] Takahashi M, Hosokoshi Y, Nakano H, Goto T and Kinoshita M 1997 *Mol. Cryst. Liq. Cryst. Sci. Technol.* A **306** 111
[20] Lake B, Cowley R A and Tennant D A 2000 *J. Phys.: Condens. Matter* **9** 10951
Garrett A W, Nagler S E, Tennant D A, Sales B C and Barnes T 1997 *Phys. Rev. Lett.* **79** 745
[21] Manaka H, Yamada I and Yamaguchi K 1997 *J. Phys. Soc. Japan* **66** 564
[22] Manaka H and Yamada I 1997 *J. Phys. Soc. Japan* **66** 1908
[23] Kodama K, Harashina H, Sakai H, Kato M, Sato M, Kakurai K and Nishi M 1999 *J. Phys. Soc. Japan* **68** 237
[24] Xu G, Broholm C, Reich D H and Adams M A 2000 *Phys. Rev. Lett.* **84** 4465
[25] Inagaki Y, Kobayashi A, Asano T, Sakon T, Kitagawa H, Motokawa M and Ajiro Y 2005 *J. Phys. Soc. Japan* **74** 2683
[26] Stone M B, Tian W, Lumsden M D, Granroth G E, Mandrus D, Chung J-H, Harrison N and Nagler S E 2007 *Phys. Rev. Lett.* **99** 087204
[27] Okamoto K 1996 *Solid State Commun.* **98** 245
[28] Ajiro Y, Asano T, Inami T, Aruga-Katori H and Goto T 1994 *J. Phys. Soc. Japan* **63** 859
[29] Gu B, Su G and Gao S 2005 *J. Phys.: Condens. Matter* **17** 6081
[30] Gu B, Su G and Gao S 2006 *Phys. Rev.* B **73** 134427
[31] Gong S-S, Gu B and Su G 2008 *Phys. Lett.* A **372** 2322
[32] Escuer A, Vicente R, El Fallah M S, Goher M A S and Mautner F A 1998 *Inorg. Chem.* **37** 4466
[33] Lu H T, Su Y H, Sun L Q, Chang J, Liu C S, Luo H G and Xiang T 2005 *Phys. Rev.* B **71** 144426
[34] Gong S-S, Gao S and Su G 2009 *Phys. Rev.* B **80** 014413

[35] Mahdavifar S and Abouie J 2011 *J. Phys.: Condens. Matter* **23** 246002
[36] Mila F 1998 *Eur. Phys. J.* B **6** 201
[37] Totsuka K 1998 *Phys. Rev.* B **57** 3454
[38] Alcaraz F C and Malvezzi A L 1995 *J. Phys. A: Math. Gen.* **28** 1521
[39] Okamoto K and Nommura K 1996 *J. Phys. A: Math. Gen.* **29** 2279
[40] Kuzmenko I and Essler F H L 2009 *Phys. Rev.* B **79** 024402
[41] Luther A and Peschel I 1975 *Phys. Rev.* B **12** 3908
[42] Cabra D C and Grynberg M D 1999 *Phys. Rev.* B **59** 119
Vekua T, Cabra D C, Dobry A, Gazza C and Poilblanc D 2006 *Phys. Rev. Lett.* **96** 117205
[43] Hikihara T and Furusaki A 2001 *Phys. Rev.* B **63** 134438
[44] Cabra D C, Honecker A and Pujol P 1998 *Phys. Rev.* B **58** 6241
[45] Japaridze G I and Nersesyan A A 1978 *JETP Lett.* **27** 334
Pokrovsky V L and Talapov A L 1979 *Phys. Rev. Lett.* **42** 65
[46] Japaridze G I, Nersesyan A A and Wiegmann P B 1984 *Nucl. Phys.* B **230** 511
[47] Dashen R F, Hasslacher B and Neveu A 1975 *Phys. Rev.* D **11** 3424
Takhtadjan A and Faddeev L D 1975 *Sov. Theor. Math. Phys.* **25** 147
[48] Zamolodchikov A B 1995 *Int. J. Mod. Phys.* A **10** 1125
[49] Zhitomirsky M E, Honecker A and Petrenko O A 2000 *Phys. Rev. Lett.* **85** 3269
[50] Hida K 1999 *Phys. Rev. Lett.* **83** 3297